3rd Middle East Turbomachinery Symposium (METS III)
15-18 February 2015 | Doha, Qatar | mets.tamu.edu

GEARBOX SUPER-SYNCHRONOUS LATERAL VIBRATION

Mr. Gaspare Maragioglio
Engineering Manager
Shaft Line Integration
GE Oil & Gas
Florence, Italy

Mr. Alessandro Pescioni
Lead Engineer
Shaft Line Integration
GE Oil & Gas
Florence, Italy

Mr. Mirko Libraschi
Senior Engineer
Advanced Technology
GE Oil & Gas
Florence, Italy

Gaspare Maragioglio is currently the Engineering Manager of the Shaft Line Integration Team for GE Oil & Gas Nuovo Pignone, in Florence, Italy. He is now responsible for technical selection and design verification of flexible and rigid couplings, load gears and auxiliary equipment, with particular focus on the train rotor-dynamic behaviour, torsional and lateral.

Alessandro Pescioni is currently a Design Engineer in the Shaft Line Integration Team for GE Oil & Gas Nuovo Pignone, in Florence, Italy. He is responsible of the requisition tasks and the integrated train rotor-dynamic studies. His responsibility includes also support to NPI, manufacturing and test department for full speed full load string test.

Mirko Libraschi is currently a Senior Engineer of the Advanced Technology Organization, for GE Oil & Gas Nuovo Pignone, in Florence, Italy. He is responsible to define and execute new technology programs. Additionally Mirko leads the technology synergies and integration across GE and Global Research Centers, to improve technology edge of Oil & Gas products.

ABSTRACT

This paper investigates gear super-synchronous vibrations experienced in turbo-compressor trains. Non-synchronous vibrations can be potentially cause of gears' damages, since they are associated to alternating torque in the shafts, thus producing fatigue stresses in the rotating equipment.

Moreover, these non-synchronous vibration components can affect the string test execution or limit the train operability at site, by bringing the overall gear shaft vibration above the acceptance values.

The phenomena analyzed in the cases studied occurred during a complete unit string test, at partial and full transmitted load, and it was observed as a harmonic excitation of the pinion shaft overhung mode (non-drive end side).

Experimental observation and comparative analysis with theoretical calculations drove the focus on the key factors which govern this phenomenon, and suggested a new approach into the train rotating components modeling procedure, in order to establish robust and reliable design tool verification.

The aim of the paper is, on the basis of string test validation, to provide:

- Direction on the train model criteria, with special attention to the gyroscopic effects of the overhung inertias and the super-synchronous bearing stiffness and damping coefficients;

- Step by step procedure to carry out the high frequency lateral rotor-dynamic analysis and to have a common base for a comparative analyses among the various cases;

- Acceptance criteria for the predictions to effectively assess gearbox rotor-dynamic behaviour and reduce the risk to have super-synchronous vibration when in operation.

The three aforementioned steps provide a sound method to assess the gear shafts' 4th lateral mode.

INTRODUCTION

A key factor to delivery first class products in the turbo-machinery application is the capability to define the optimum shaft line architecture for the required duty, in an integrated system environment.

The single pieces of rotating equipment can exhibit satisfactory rotor-dynamic behavior during the Factory Acceptance Test (FAT), when in a standalone configuration, but this cannot always be considered representative to the real operating conditions in the site service.

In particular for the gearboxes, the mechanical running test at the manufacturer's workshop, as required by the API613, is able to capture only the macroscopic non conformities and their basic rotor-dynamic behavior. In fact, being the gearbox a load dependent piece of the rotating equipment, its dynamic behavior is heavily affected by the balance between the internal forces (shafts weight and transmitted torque) and the external forces applied to the shafts. At the gear manufacturer's workshop the typical maximum applicable load is roughly 800kW, so for the multi megawatt machines the applied loads are nowhere near sufficient to replicate the actual operating conditions in the journal bearings or the tooth contact. Moreover the only external forces applied to the gearbox during the FAT are the overhung weights of the job couplings moment simulators.

Much more significant is the contribution that the string test can provide in understanding the gear behavior at site configuration when operating at full speed and full load.

The material presented in this paper is based on the outcomes of a complete unit string test carried out for a Methane LNG project, here after identified as the case "C", and their correlation with the associated rotor-dynamic analytical studies. The intention is also to present the most recent experience obtained by authors in the area of gear super-synchronous lateral vibration, observed in turbo-compressor trains. The results will give wide and deep understanding of the subject.

Case "C" project overview

The project is one of the latest Australian mega-projects to liquefy the natural gas (LNG), which includes the extraction of the coal seam gas, the gas transmission pipeline and a the LNG Facility composed by the trains Propane, Ethylene and Methane (the arrangement of Methane train is shown in Figure 1).

Case "C" string test arrangement and execution

The Methane train package was erected on a dedicated test bench at the manufacturer plant. The installation included all the auxiliaries, base-frame and structures to be used in operation at site. In the previous individual tests each of the sub-components has been validated by the Factory Acceptance Test at the manufacturer's works, in accordance to the API Standards.

The purpose of the string test was to demonstrate the mechanical integrity and efficiency of the integrated shaft-line and the aerodynamic stability of the compressors, in the specified operating conditions, as well as to validate the rotor-dynamic performances of the rotating equipment.

Summary of the tests:

a) Full Speed, Full Load, Full Pressure complete unit test (the compressors performance curves have been explored during the test run) – a torquemeter installed on load coupling measured the driver rated power;
b) Lube Oil Temperature Variation test from 50°C to 60°C.

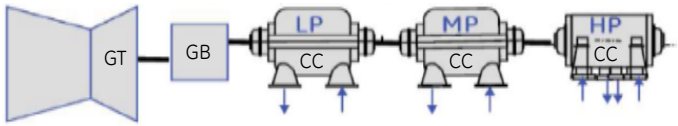

Figure 1 – Methane train arrangement

MOTIVATION FOR STUDY AND APPROACH

Moved by the lessons learnt during the full speed full load test of the case "C", the paper collects also the experience of the following cases, which are listed in the Table 1, in a chronological order.

In all these cases the turbo-machinery train was equipped with an API613 speed increasing gearbox, double helix and horizontal offset, tilting pad journal bearings on the HSS and thrust bearing on the LSS. The gearboxes are defined as high energy gears, due to the combination of pitch line velocity and transmitted torque. The power transmission was realized through the flexible couplings, diaphragm and disc types.

	Train Composition	Rated Power (kW)	HSS Speed Range	HSS bearings	Speed Ratio	PLV (m/s)	L/D
Case "A"	GT-GB-CC-CC	33,500	10,829 rpm 70-105%	TPJ	1.78	184	1.72
Case "B"	GT-GB-CC	23,500	10,617 rpm 70-105%	TPJ	1.63	173	1.59
Case "C"	GT-GB-CC-CC-CC	36,670	6,068 rpm 85-105%	TPJ	1.69	138	1.44
Case "D"	GT-GB-CC	35,000	10,981 rpm 70-105%	TPJ	2.35	174	1.95
Case "E"	GT-GB-CC	32,561	9,281 rpm 70-105%	TPJ	1.52	171	1.58
Case "F"	GT-GB-CC-CC-CC	48,200	5,940 rpm 85-105%	TPJ	1.65	143	1.64

Table 1 - Case Studies

THE STATE OF ART

This section provides a summary of the experiences precedent to the case "C" (cases "A" and "B"), as well as the cases available in literature. The presentation format for each case is: problem statement – phenomenon identification – corrective actions.

The string test observations, relative to the cases "D", "E" and "F", are reported as part of the conclusion in order to support and validate the new criteria proposed by this paper in terms of system modelling and results acceptability. For reference it can be noted that all the three cases have been analyzed using the new proposed method, and the outcomes of the full load string tests, successfully completed without any vibration issues, confirmed the prediction of the theoretical calculations.

Case "A" - Problem statement

The gearbox vibration on NDE pinion bearing increases when the power exceeds 18MW @ 100% speed (reached 45÷50µm p-p @ 10,830 rpm and 23MW). The main vibration component is the 7X speed harmonic, observed 17.5µm p-p at 1,262 Hz, as shown in Figure 2.

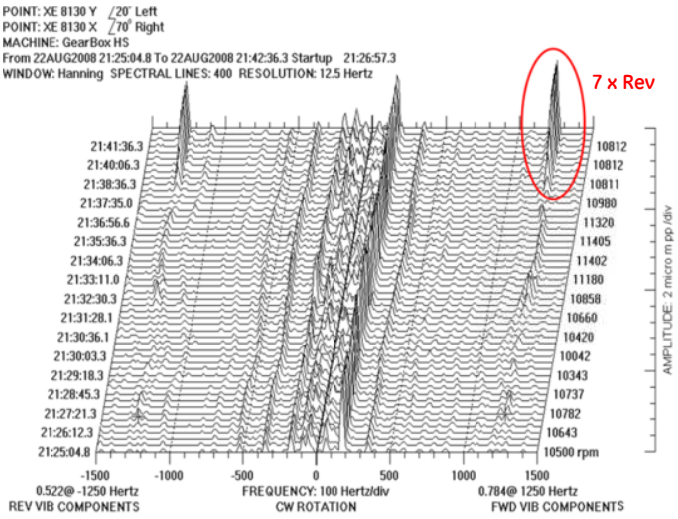

Figure 2 - Case "A" vibration Waterfall HSS NDE

Case "A" - Phenomenon identification

The super-synchronous lateral analysis confirmed the pinion shaft overhung lateral natural mode at 75,117 cpm, with a poor damping capability, LogDec 0.24 (see Figure 3).

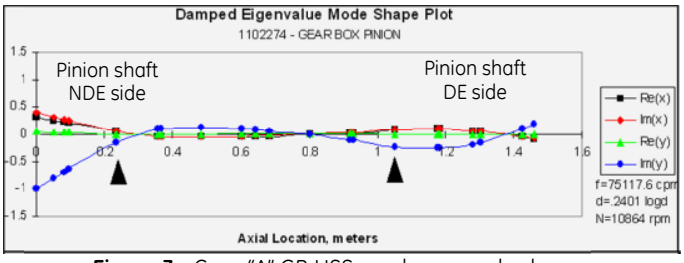

Figure 3 - Case "A" GB HSS overhung mode shape

Case "A" - Corrective actions

Installation of fixed profile journal bearings, offset halves type, with pressure dam on gear pinion shaft (the original journal bearings were TPJ type); this solution was validated by the calculation, which highlighted an increase of the system damping at the frequency of interest.

The experimental outcomes, observed during the full load string test, confirmed the expected rotor-dynamic improvements.

Case "B" - Problem statement

An high vibration was observed during the string test at a certain combination of speed and load on the gearbox pinion shaft, specifically at the non-drive end side. At the maximum continuous speed (11,157 rpm) the super-synchronous vibration is activated at roughly 14MW, the excited frequency is ~1,300Hz, corresponding to the 7X speed harmonic. At lower shaft rotational speed the super-synchronous vibration is detected at 8X speed harmonic (see Figure 4).

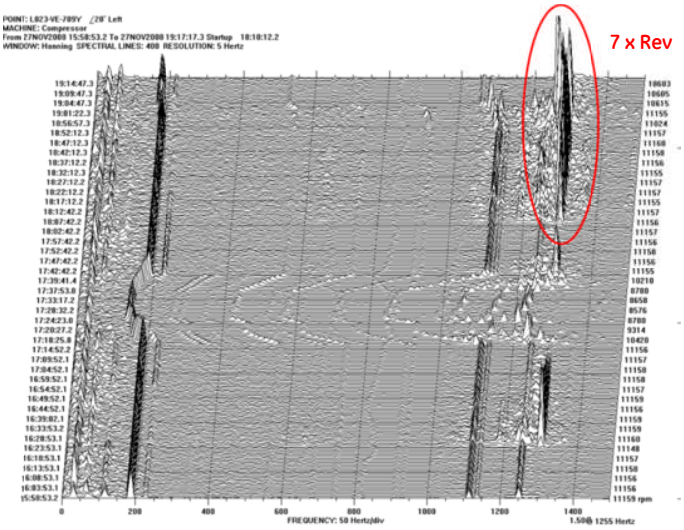

Figure 4 - Case "B" vibration Waterfall HSS NDE

Case "B" - Phenomenon identification

The calculations again confirmed the correlation between the observed super-synchronous vibration

frequency and the pinion shaft overhung lateral natural frequency. In this case the analytical calculation also highlights a very poor system damping in the original design, LogDec 0.0044 (see Figure 5).

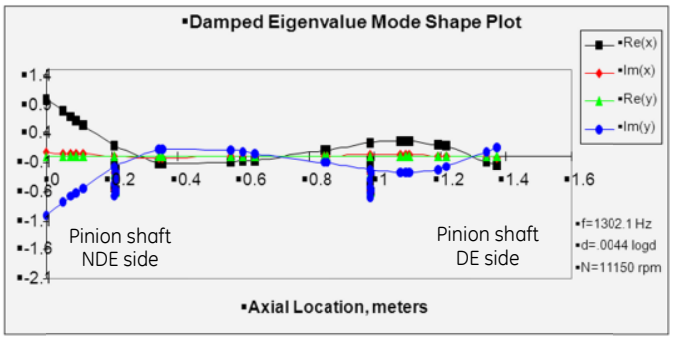

Figure 5 - Case "B" GB HSS overhung mode shape

Case "B" - Corrective actions

Special fixed profile journal bearings, offset halves type, with pressure dam, have been designed and installed on the gear high speed shaft (the original bearing were TPJ type). These bearings have been optimized to increase the damping; moreover the position of the NDE bearing was shifted toward the NDE side by 13 mm to locate the bearing in the section with major shaft motion.

The string test observations, at the various speed and load conditions, demonstrated again the improved performances obtained with the corrective actions.

Cases available in literature

Memmott [1] details that in three separate turbo-compressor trains, a gear pinion shaft modification was required to solve the super-synchronous vibration issues observed during the full speed - full load string tests. Two trains were driven by a project gas turbine and one by a shop steam turbine. The power to drive the compressor ranged from 16.18 MW to 22.84 MW; in the three instances, the gear design was a double helix, single stage, with a speed ratio ranging from 2.14 to 2.44, and tilting pad bearings on the high speed shaft.

The frequency of concern was eight times the pinion shaft running speed (8XRev), and it was observed only at load condition. The super-synchronous frequency coincided with the shaft fourth lateral natural frequency (for these three cases the speed of gear pinion shaft was respectively: 10,780 rpm – 11,608 rpm – 12,304 rpm).

Memmott [1] states that the first pinion was modified by removing weight from the non-drive end side, and the other two pinions were modified by adding weight to the non-drive end side. The modifications aimed to move the aforementioned lateral natural frequency out of the excitation range with the 8X speed harmonic.

CASE "C" PROBLEM STATEMENT

During the internal FSFL test of the Methane train, a super-synchronous vibration component was observed on the gear pinion shaft NDE side; the vibration phenomenon was also captured by the gear casing accelerometers.

Figure 6 shows the vibration trend and spectra recorded by a displacement sensor HSS NDE "Y". A similar vibration was observed along the "X" direction, but omitted for brevity. At the time frame highlighted by the red circle (Figure 6), the excited frequency is ~955 Hz, with a transmitted load of 19.2 MW and a rotor speed of 5,170 rpm. Consequently, the excitation mechanism is realized with the 11X speed harmonic.

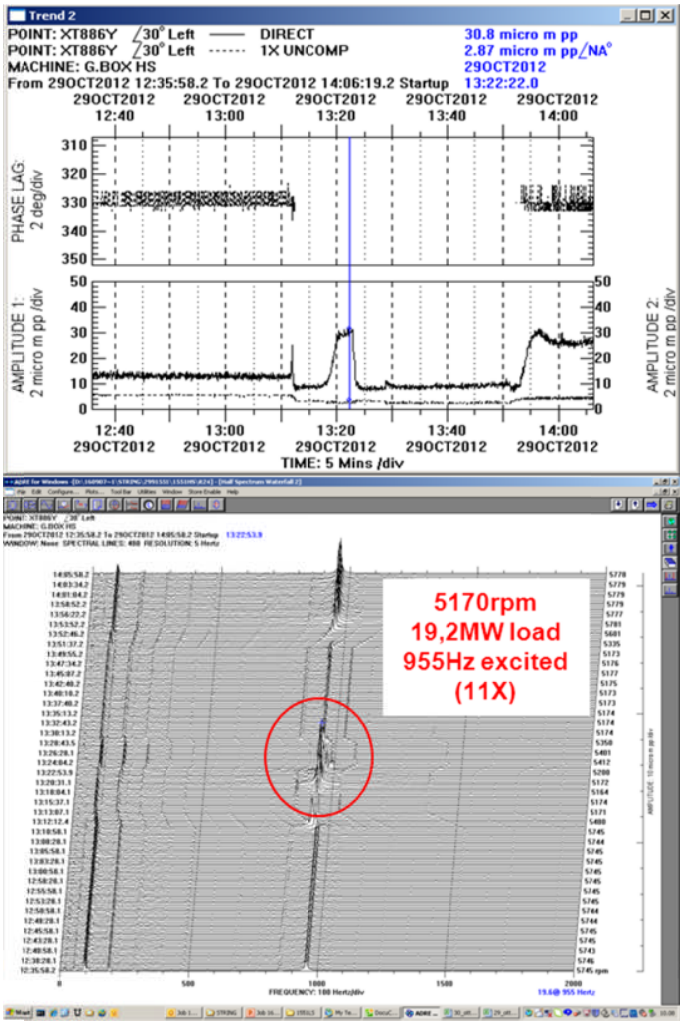

Figure 6 - Trend and Waterfall HSS NDE "Y" – 5,170 rpm

The vibration became prevalent at a specific combination of speed and load, and showed a full repeatability in the load dependence:

- At the speed where this phenomenon occurred, the vibration amplitude increased with the load. Keeping fixed the operating speed and increasing the transmitted torque, an increase in the amplitude of super-synchronous vibration response occurred.
- The lube oil inlet temperature did affect the vibration behavior. With the lube oil inlet temperature at 50°C, and at the MCS, the super-synchronous vibration appeared at 24-25 MW, and later disappeared at full load operation. With the lube oil inlet temperature at 60°C, the vibration component persisted up to the full load condition.
- Variation in the lube oil flow and pressure influenced little the amplitude of the super-synchronous shaft vibration.

The Figure 7 depicts the super-synchronous vibration at 5,776 rpm and 23.9 MW. In this case the 10X speed harmonic excites the ~965 Hz. In both cases the observed frequency was recognized as the gear pinion shaft fourth lateral mode; the phenomenon mainly involved the pinion shaft NDE side, in accordance to the relevant mode shape.

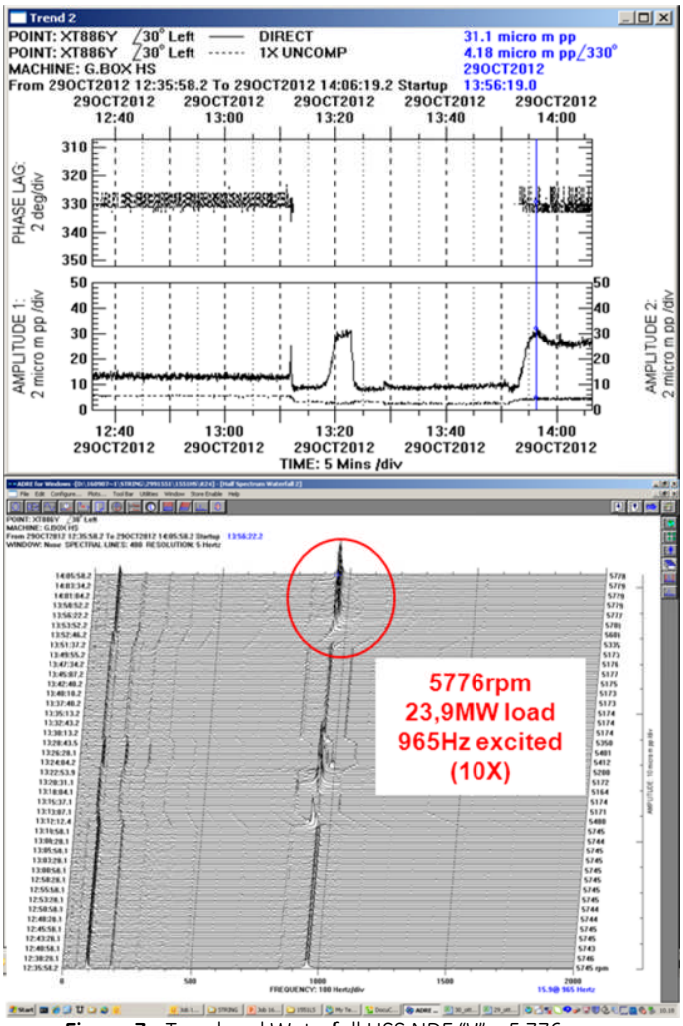

Figure 7 - Trend and Waterfall HSS NDE "Y" – 5,776 rpm

The overall vibration was always well within the alarm threshold (51 µm p-p), however under some conditions it exceeded the string acceptance criterion of 35 µm p-p, and therefore it jeopardized the performance test. The main vibration contributor was the component at ~950÷965Hz. The observed vibration frequency slightly varied versus the speed and load conditions, this was due to the effects that these parameters (transmitted power and speed) have on the journal bearings force coefficients.

CASE "C" RCA

To establish the root cause of the gear vibration is required to identify the following:

- *Excitation Mechanism = relation between cause and effects;*
- *Excitation Source = location of excitation origin;*
- *Excitation Function = deviation that produces the excitation;*

The excitation mechanism that results in the super-synchronous phenomenon is well understood.
The pinion shaft fourth lateral mode is excited by the gear rotational speed harmonics.
The excitation speeds can be defined as those speeds at which the super synchronous vibration is activated by one or more gear rotational speed harmonics that occur within the compressor operating speed range. These excitation speeds are identified by dividing the pinion 4th lateral natural frequency by the relevant shaft rotation speed harmonics, 9X, 10X and 11X.

Inevitably the exact calculation of the excitation speeds is affected by the uncertainty due to the acquisition system resolution:

	MCS	100%	MOS
Operating speed (rpm)	6,371	6,068	5,158
Observed Frequency		950Hz	
Speed harmonic	9X	10X	11X
Excitation speed (rpm)	6,333	5,700	5,182

In other words, at the mentioned excitation speeds, the harmonics 9X, 10X and 11X excite the pinion shaft overhung mode, based on the energy available into the system. All these three speeds are in the compressors operative speed range (5,158÷6,371 rpm).

Most likely the excitation source is located at the gear mesh, and this can be demonstrated by observing the vibration spectrum captured during the gear FSNL test at the gearbox manufacturer's workshop (see Figure 8). In fact, during this test there were no external forces similar to those applied in the string test arrangement, but the spectrum clearly shows several speed harmonics components. These components were to be observed later during the full load string test.

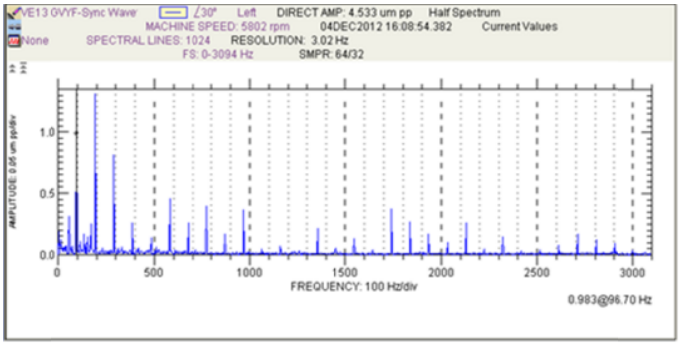

Figure 8 - Vibration Spectrum HSS NDE "Y" @ 5,800 rpm

This observation indicates that the excitation source is located within the gearbox and as the vibration response depends on the transmitted torque, it shows a relationship with the teeth meshing mechanism.

Unfortunately, the excitation forces originated into the meshing, due to the transmission errors, are difficult to be identified. In fact, the dynamics of the mesh are non-linear and are heavily influenced by many factors, namely:

- Total helix deviation;
- Total profile deviation;
- Tooth-to tooth pitch deviation;
- Total pitch deviation;
- Cumulative pitch error;

The transmission errors are due to the difference between the actual position of the output gear and the position it would occupy if the gear drive were perfectly conjugated.
In general the gear transmission errors are the most likely excitation function for high frequency vibration. Excitations as a multiple of running speed are very likely to occur in a geared system.

If the excitation function is not well understood and quantified, it cannot be removed, and therefore the gear shafts 4th lateral mode shall be properly damped to avoid dangerous super-synchronous vibration. In the past the OEM proposed a way to assess the gear shafts high frequency modes, providing the LogDec threshold that defines the critical area, where it is required to carry out a super-synchronous rotor response analysis, or the confidence area, where no super-synchronous vibration components are expected.

The aforementioned criteria, based on the previous lessons learnt (see cases "A" and "B" in table 1), failed to predict the critical lateral behavior of the gear pinion shaft, case "C". This is because the super-synchronous analysis carried out by the gearbox manufacturer overestimated the system damping (the actual LogDec was smaller than the LogDec predicted in the original analysis). The difference was due to the incorrect rotor-bearings model; in particular the main contributing error arising from the use of synchronous bearing stiffness and damping coefficients (for all the studied cases, at different bearings clearances and load conditions, the predicted LogDec was above 0.8).

BASE LINE ANALYSIS – ORIGINAL DESIGN

The super-synchronous study of pinion shaft, case "C", as well as those of the other cases, were carried out using Timoshenko beams, with gyroscopic effects in a component mode synthesis analysis using a commercial rotor-dynamics software (the original pinion design is shown in Figure 9).

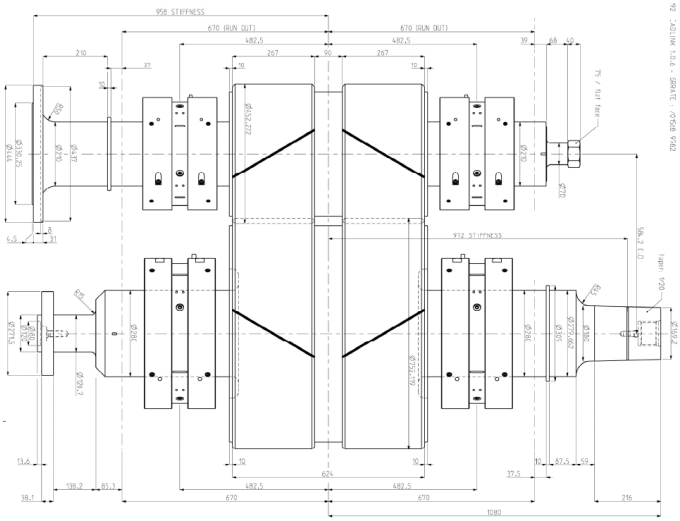

Figure 9 – Original pinion design

The Figure 10 shows the structural beam model which was tuned to match the first two free-free shaft modes as determined by a full FEM analysis using 3D solid elements (the FEM is shown in Figure 11).

The tuning was made by adjusting the separation line angle between two layers of the same element (gear body), one of these having only mass properties and the other one having mass and elastic properties.

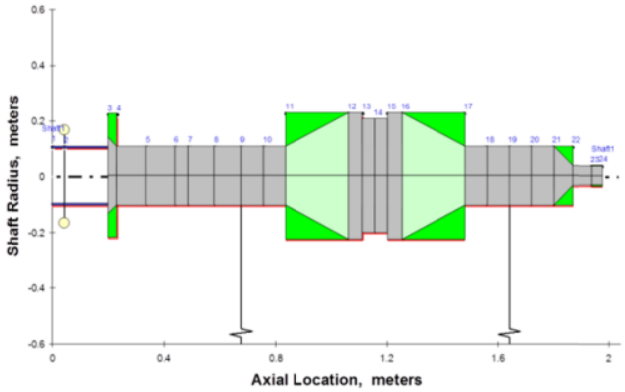

Figure 10 - Pinion shaft beam model

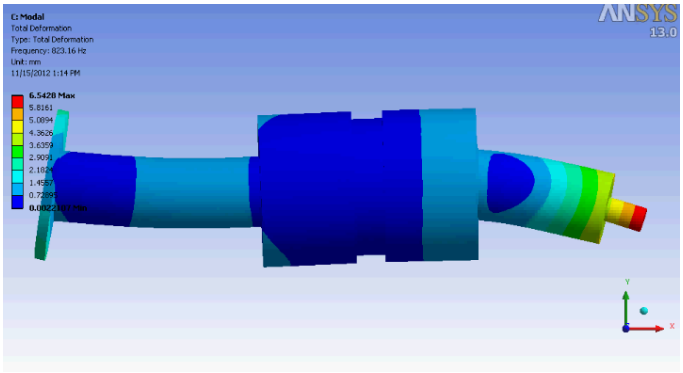

Figure 11 - Pinion shaft FEM model

The modeling of the flexible coupling between the gearbox and the centrifugal compressor was added to the system and fully accounting for the gyroscopic effects, which play a fundamental role into the gear super-synchronous lateral mode frequencies definition. The coupling transverse and polar moment of inertia were identified through an ANSYS model of the component (see Figure 12).

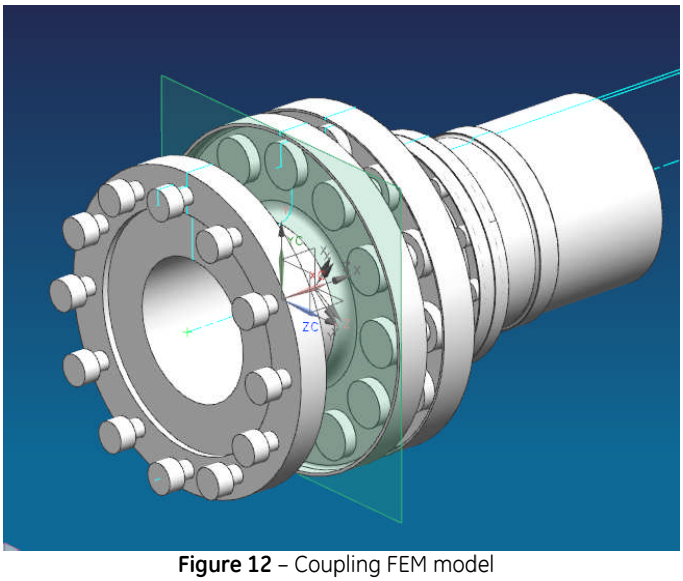

Figure 12 – Coupling FEM model

To establish a sensitivity on the tilting pad bearing force coefficients, these were calculated with and without the effects of the pad thermo-mechanical deformation, but always considering the pivot flexibility. In Figure 13, it can be observed the impact of the pad thermo-mechanical deformation on the bearing direct stiffness. This deformation tends to increase the direct stiffness by decreasing the bearing clearance (thermal effect) and by increasing the preload (mechanical effect).

The rotor-dynamic code calculates the complex eigenvalues of the rotor-bearing system, using the component model synthesis (CMS). Four degrees of freedom per node are considered (axial constrain). The eigenvalues are obtained in the state space of the linearized system.

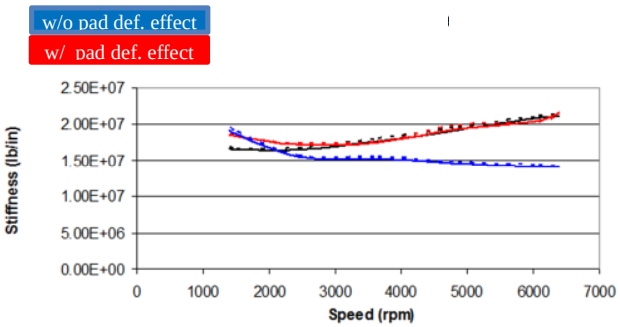

Figure 13 - TPJ Direct Stiffness

The undamped critical speed map shown in Figure 14, highlights the intersection between the system lateral critical speeds and the aforementioned bearing direct stiffnesses, with and w/o the pad deformation effect.

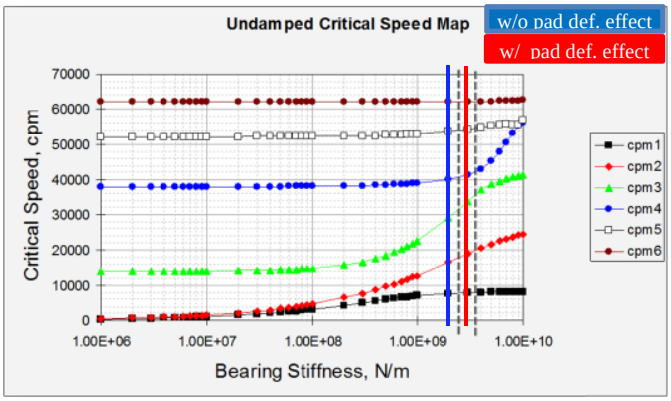

Figure 14 - Original pinion UCS

The figures 15 and 16 depict the rotor mode shape the and LogDec for the 4th lateral dumped mode. When considering the pad thermo-mechanical deformation, the LogDec decreases from 0.95 (see Figure 15) to 0.58 (see Figure 16).

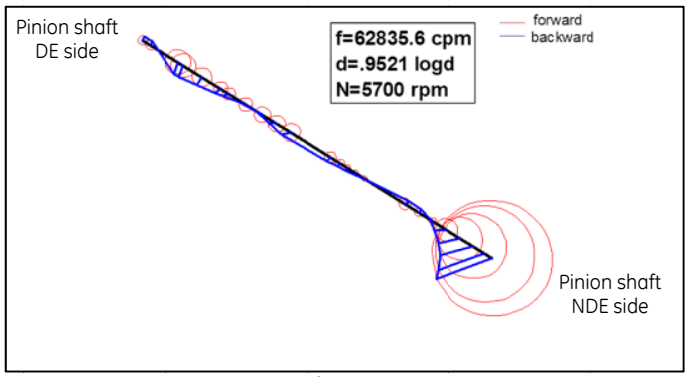

Figure 15 –HSS mode shape w/o thermo-mechanical deformation

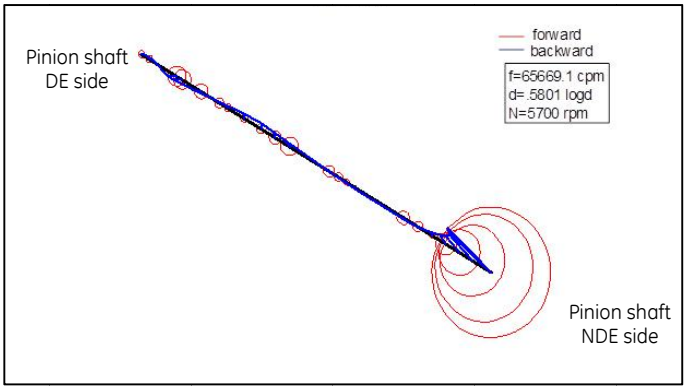

Figure 16 – HSS mode shape with thermo-mechanical deformation

In addition to the bearing direct stiffness, the effective damping determined by the bearings cross coupling stiffness coefficients also affects the system overall LogDec. The aforementioned coefficients represent the tangential forces acting to the shaft as shown on the schematic sketch presented in the Figure 17.

$$C_{eff} = C_{net}\left(1 - \frac{k_{net}}{C_{net}\cdot\Omega}\right) \quad (1)$$

Where $C_{net}=C_{xx}+C_{yy}$ and $k_{net}=k_{xy}-k_{yx}$.

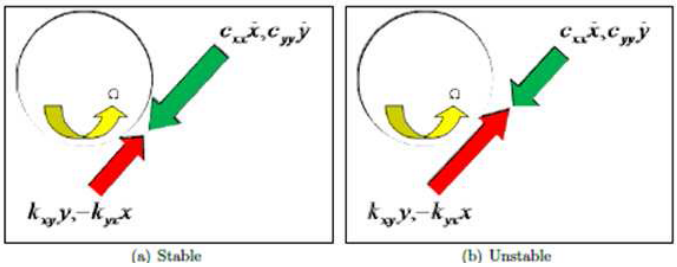

Figure 17 – Tangential forces to shaft (stable/unstable condition)

The bearings a-synchronous coefficients calculation is carried out in an iterative process. The first step consists of calculating the coefficients at the frequency of interest. These coefficients are then successively used to re-define the complex eigenvalues, and therefore to obtain the asynchronous bearing coefficients at the new frequency. This procedure is repeated until there is a negligible variation in the resulting 4th mode frequency.
As depicted in Figure 18, considering the super-synchronous reduced coefficients, the cross coupling terms increase by four times respect those obtained by using the synchronous reduced coefficients (while no significant changes result in the direct terms).

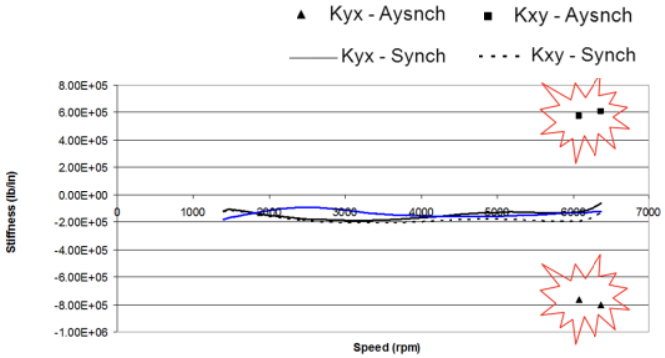

Figure 18 - TPJ quadrature stiffness vs shaft speed

Moreover, while the absolute values of cross coupling stiffness increase at the specified frequency, the direct damping terms do not increase, and therefore the ratio between k_{net} and C_{net} keeps increasing. It is possible to represent this behaviour with a whirl frequency ratio (WFR) defined as:

$$WFR(\Omega) = \frac{k_{net}}{C_{net}\cdot\Omega} \quad (2)$$

The WFR value, linked to the system effective damping, represents physically the pad ability to adapt its position to the oil film, and at high frequency the pad inertia reduces its capacity to follow the shaft vibration. This explains why an increase of the WFR leads to a corresponding decrease of the system LogDec. In particular, considering for the case "C" the super-synchronous coefficients, the WFR increases up to 0.21, and this leads the tilting pad bearing to behave like a fixed geometry bearing, with a consequent increasing of the tangential forces, and therefore of the system instability (WFR≈0.5).
Nevertheless, the fixed geometry bearings can be designed to invert the scenario, providing special features to decrease the WFR; and consequently to increase the stability at high frequency modifying the direct stiffness (K) and damping (C) coefficients, like in the cases "A" and "B". Of course, this depends on the bearing manufacturer capability to optimize the geometry towards improved damping at the super-synchronous frequency.

Using the asynchronous coefficients the LogDec of gear pinion shaft 4th lateral mode decreases even more. With respect to the case shown in Figure 16, the LogDec reduces down to 0.18, as shown in Figure 19.
Based on the collected experience, the LogDec 0.18 is considered inadequate to provide the required modal damping. In fact, the gear pinion shaft 4th eigenvalue, shall not be evaluated as a self-excited mode (critical when LogDec <0.1), but as a forced excited mode with an excitation originated into the gear mesh.

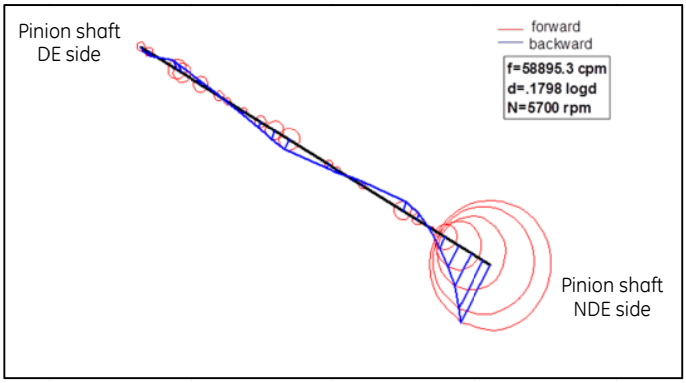

Figure 19 – HSS mode shape with a-synchronous coefficients

Finally the vibration at the pinion shaft 4th lateral frequency depends on the presence of the excitation force, by its amplitude, and by the system modal damping.
Unfortunately, due to the uncertainties on the excitation function, and therefore due to the difficulties to define its amplitude versus the gear teeth geometrical deviations, the super-synchronous rotor response analysis can be carried out only on hypothetical basis, and so it cannot be considered representative of the actual system behaviour.
The ultimate postulate is that in case the "C" the external energy arising from the gear meshing was sufficient in amplitude to excite this mode due to its low level of modal damping.

ORIGINAL DESIGN - EXPERIMENTAL RESULTS

The string test observations for the case "C" original design are consistent with the base-line predictions, thus confirming the validity of the calculations when the a-synchronous bearing coefficients are used.

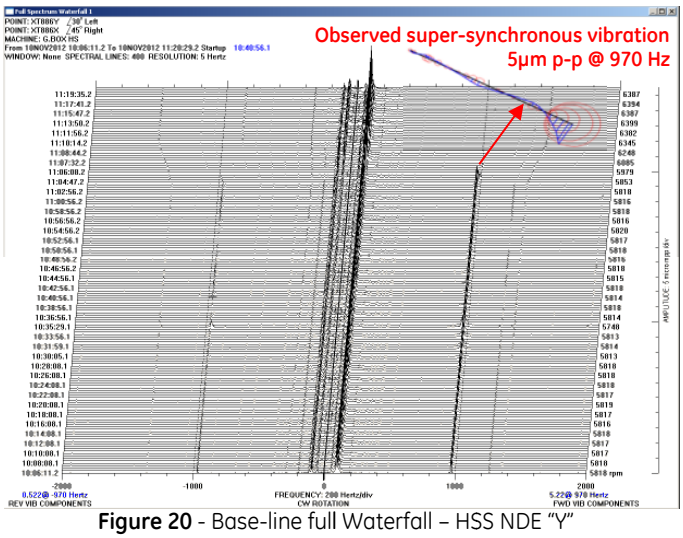

Figure 20 - Base-line full Waterfall – HSS NDE "Y"

Unfortunately the risk of super-synchronous vibration was not captured during the gearbox design stage because the original pinion shaft 4th mode analysis provided erroneous LogDec values, which were in the area of confidence (i.e. too high and overly optimistic).
The Figure 20 shows the recorded spectra of the original pinion shaft vibration behaviour. The observed super-synchronous component is 970 Hz, roughly 1% lower than the predicted frequency of the pinion shaft 4th lateral mode, with the same forward whirl (see the prediction shown in Figure 19).

As described in the section "*problem statement*", the super-synchronous vibration component brought the overall pinion shaft vibration above the string acceptance criteria (in some conditions this component exceeded 20µm p-p).

MODIFIED ROTOR ANALYSIS

The new modeling criteria were adopted to define the corrective actions needed to reduce the amplitude of the super-synchronous vibrations. These criteria are part of the novel proposed method of analysis; in particular the rotor-bearing system is modeled as described below:

- The shaft beam model is tuned according to the FEM outcomes;
- The coupling components are modeled separately, including the flexible element; the polar and transversal moment of inertia are those defined by FEM;
- The bearing's damping and stiffness coefficients are calculated at the frequency of the observed phenomenon (asynchronous coefficients); the overhung lateral mode analysis and LogDec definition are performed through an iterative cycle of calculation, updating each time the asynchronous coefficients, depending on the new mode frequency until an appropriate convergence is reached;

According to the past experiences, and the cases available in literature, a series of gear design changes were analyzed in order to define the optimum compromise to avoid the excitation mechanism (in the case "C" the active speed harmonics were known), or to increase the system modal damping. For each of these design changes a sensitivity analysis was carried out, to identify the most effective parameters.

A summary of the cases studied follows:

- Bearing substitution with fixed profile and pressure dam configuration.
- Bearing span change (move the NDE bearing closer to the shaft major motion area).
- Bearing clearances and pre-load modification.
- Pinion shaft NDE, mass increase/decrease.

Due to the limited number of the design solutions proposed by the bearing manufacturer, none of the cases with modified bearings was able to provide the sufficient beneficial results in terms of system modal damping.

Therefore the analysis focused on the pinion shaft design modification. The solution finally adopted relates to the shaft mass reduction, and was realized by drilling a bore on the NDE side of the pinion shaft (see the shaft drawing details in Figure 21 and the shaft model details in Figure 22).

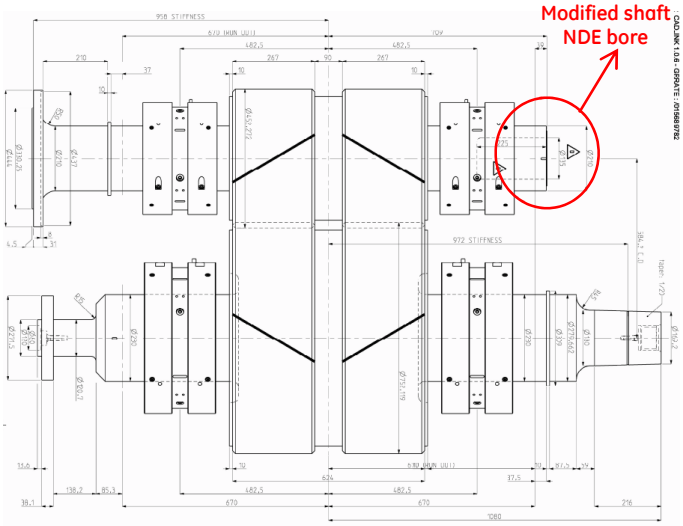

Figure 21 - Modified pinion shaft design – NDE bored

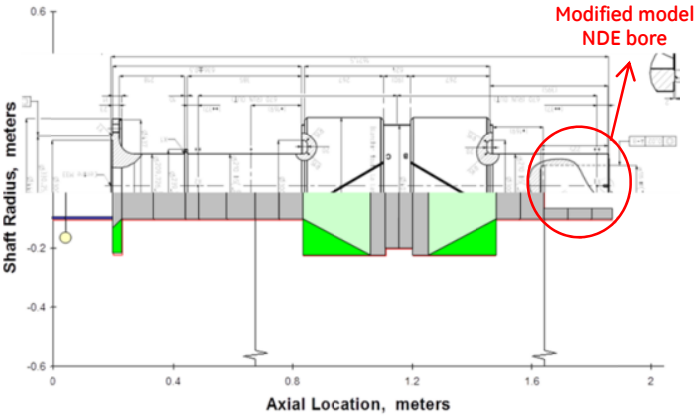

Figure 22 - Modified pinion shaft beam model

With the aforementioned corrective action, the expected benefits are:

- Reduction of the modal mass participation to the NDE mode, increasing the associated frequency and avoiding the excitation mechanism at the observed 9X and 11X speed harmonics, even if it was not possible to eliminate the excitation with the 10X or with higher order of speed harmonics.
- Change the modal shape, with the bearing center line located far away from a nodal point, and therefore to increase its damping capability.

Modified Pinion Shaft – Results of Analysis

As expected the undamped critical speed map (see Figure 23), highlighted an increase of the pinion overhung mode frequency (white and brown curves). This is a partial result as the contribution of the bearings damping was not yet included in the model.

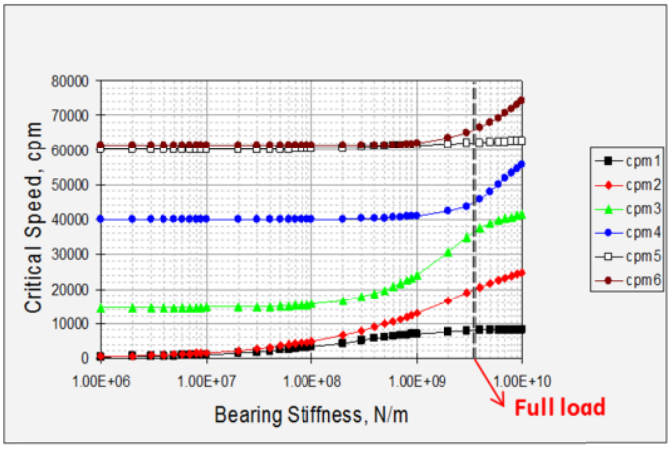

Figure 23 – Modified pinion - UCS (no damping)

In fact, the damped eigenvalues analysis shows a further increasing of the overhung mode frequency, now above 70 kCPM, as it can be clearly observed on the Campbell diagram depicted in Figure 24.

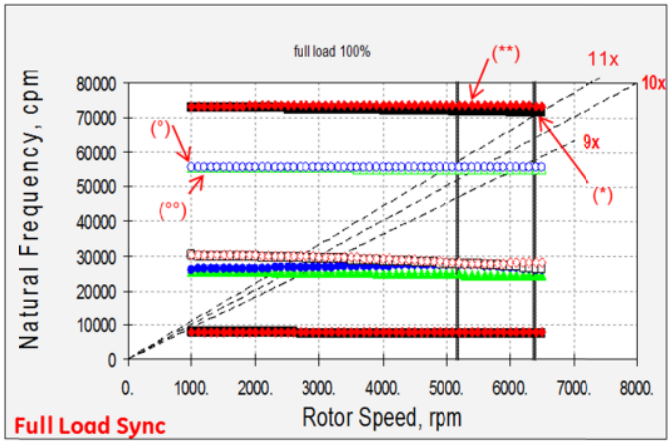

Figure 24 – Modified pinion – Campbell
(Damped analysis with synchronous bearing coefficients)

The Campbell diagram in Figure 24 is determined using the bearing coefficients evaluated at the synchronous speed frequency. Next step into the pinion shaft lateral study is the damped eigenvalue calculation using the a-synchronous bearing coefficients.

The Figures 25÷28 show the mode shape, frequency and LogDec of each lateral mode identified with the symbols (°), (°°), (*), (**) in Figure 24, using the a-synchronous coefficients. The mentioned lateral modes are those of interest, according to what observed during the string test in terms of frequency and shaft location (the super-synchronous vibration was observed on the pinion shaft NDE side).

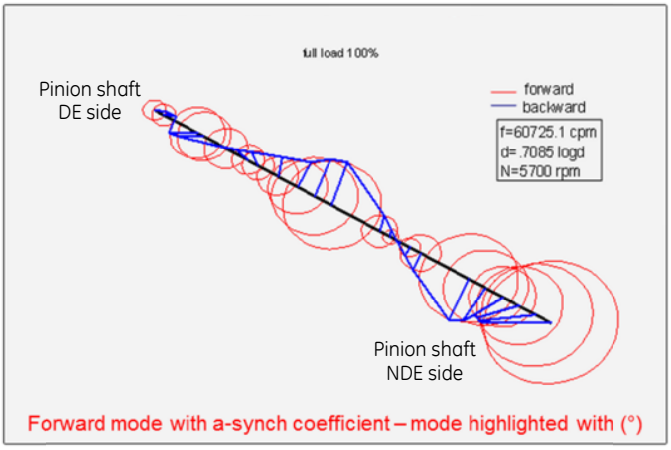

Figure 25 – Modified pinion – Mode Shape (°) @ 5,700 rpm

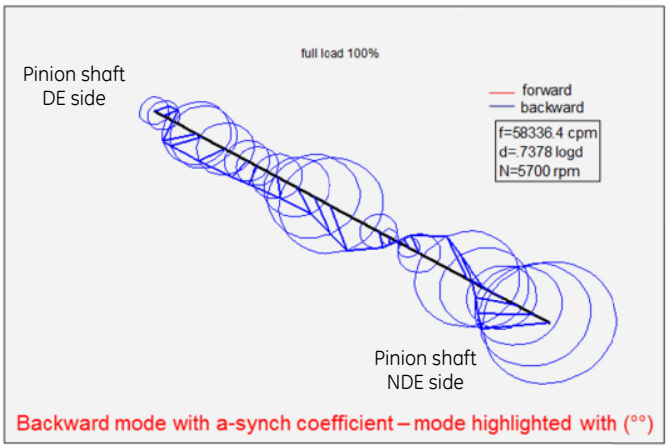

Figure 26 – Modified pinion – Mode Shape (°°) @ 5,700 rpm

Respect to the original pinion shaft design (see the mode shape and LogDec in Figure 19), the pure shaft overhung modes are now shifted above 74 kcpm, with an increased LogDec as shown in Figures 27 and 28.

The modes marked with the symbols (°) and (°°) fall now in the frequency range of the previous test observation (55-60 kcpm), they involve the whole pinion shaft but now with an adeguate LogDec up to 0.7 and 0.73 respectively.

Figures 29÷32 show the results of the a-synchronous analysis carried out at partial load condition, using a recalculated set of bearings coefficients.

The aforementioned partial load condition is 50% of gear rated power, corresponding to the compressors nominal absorbed power at 5,700rpm, so it represents the most realistic condition for a comparison with the test vibration outcomes.

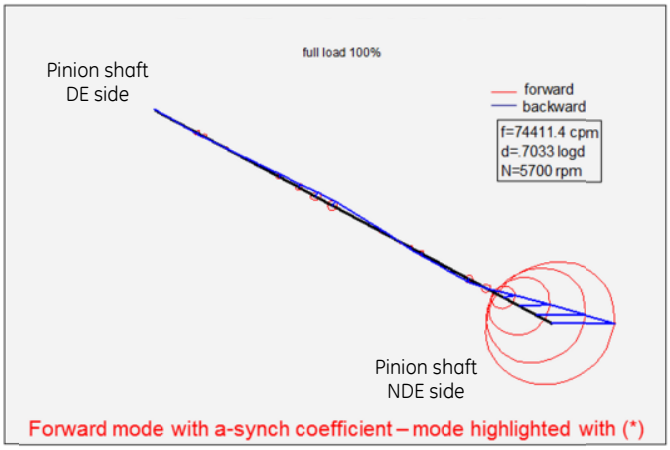

Figure 27 – Modified pinion – Mode Shape (*) @ 5,700 rpm

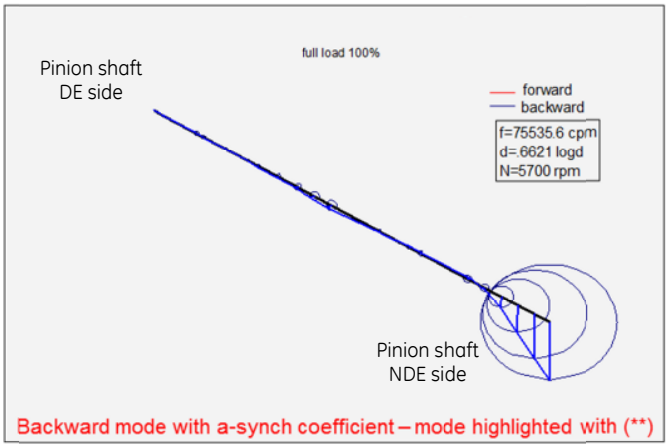

Figure 28 - Modified pinion – Mode Shape (**) @ 5,700 rpm

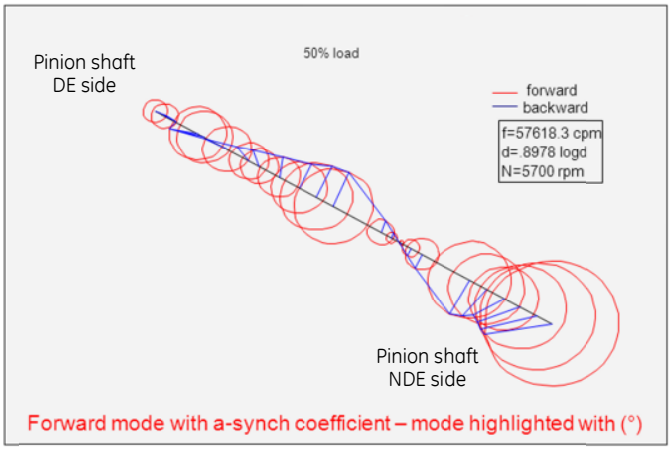

Figure 29 - Modified pinion – Mode Shape (°) @ 5,700 rpm, 50% load

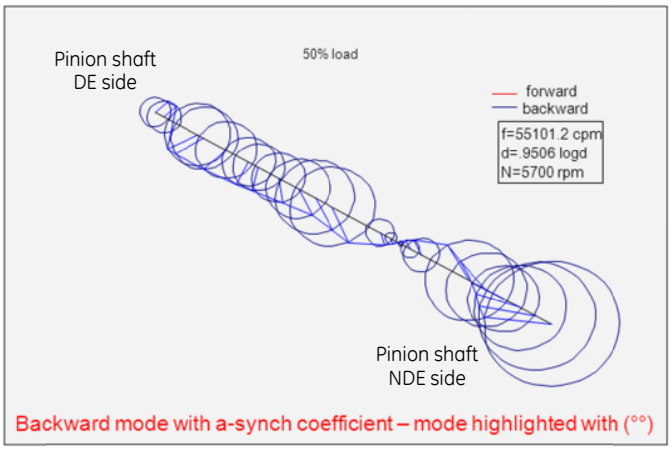

Figure 30 - Modified pinion – Mode Shape (°°)@5,700 rpm, 50% load

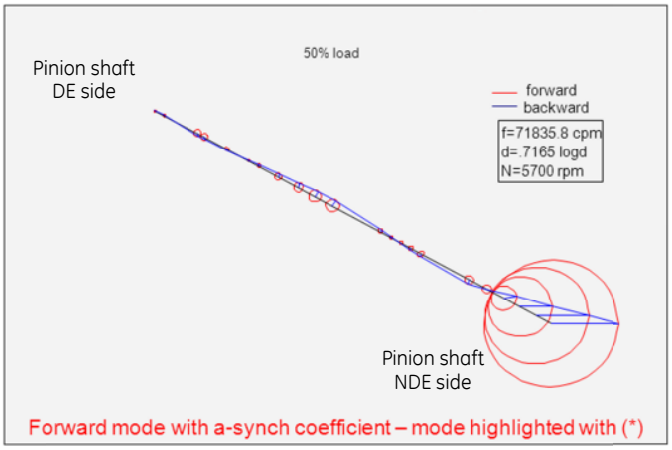

Figure 31 - Modified pinion – Mode Shape (*)@5,700 rpm, 50% load

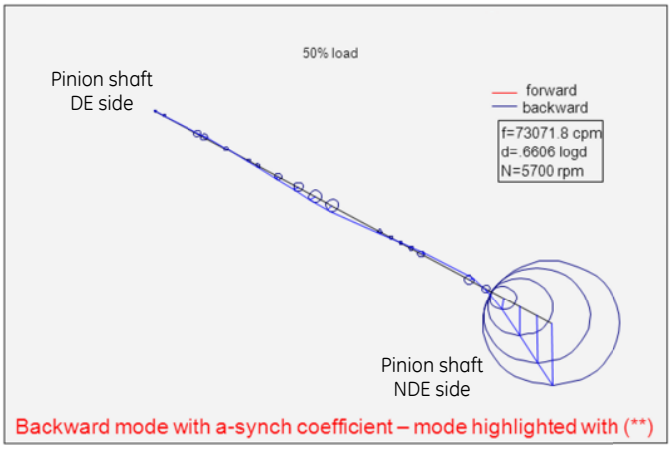

Figure 32 - Modified pinion – Mode Shape (**)@5,700rpm, 50% load

At partial load (reduced transmitted power) it is observed a general reduction of the modes frequency and a general increase of their modal damping.

MODIFIED PINION SHAFT - EXPERIMENTAL RESULTS

The new string test carried out to validate the adopted corrective action (pinion shaft NDE modification) confirms the improved shaft vibration behavior, with the overall shaft vibration well below the acceptance criteria of 35 µm in all operating conditions. The figures 33 and 34 show the pinion shaft vibration trends, with a maximum direct vibration of 16 µm p-p.

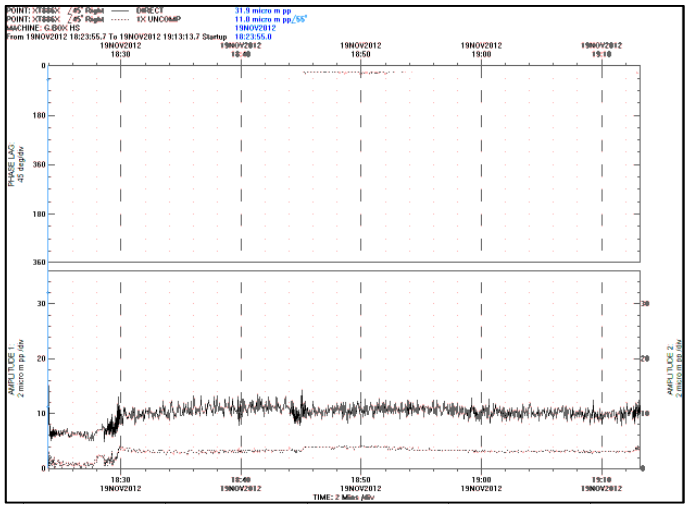

Figure 33 –Modified pinion – Measured vibration @ NDE "X"

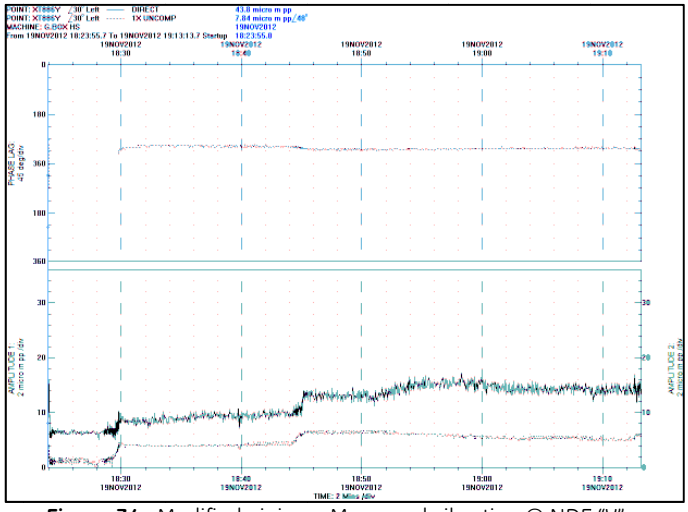

Figure 34 –Modified pinion – Measured vibration @ NDE "Y"

As shown in Figure 35, the super synchronous vibration component is still present at 970 Hz (10X speed harmonic), demonstrating the good correlation with the prediction: the calculated frequency of mode (°) is 57,618 cpm (see Figure 29) i.e. 960.3 Hz, so roughly 1% less of that measured. Considering the acquisition system frequency resolution and the very high frequency of the studied phenomenon, the calculation can be considered very accurate.

The results are in line with the corrective action purpose, which was aimed to increase the system modal damping and avoid the intersection with the 9X and 11X speed harmonics, not to remove the excitation function.

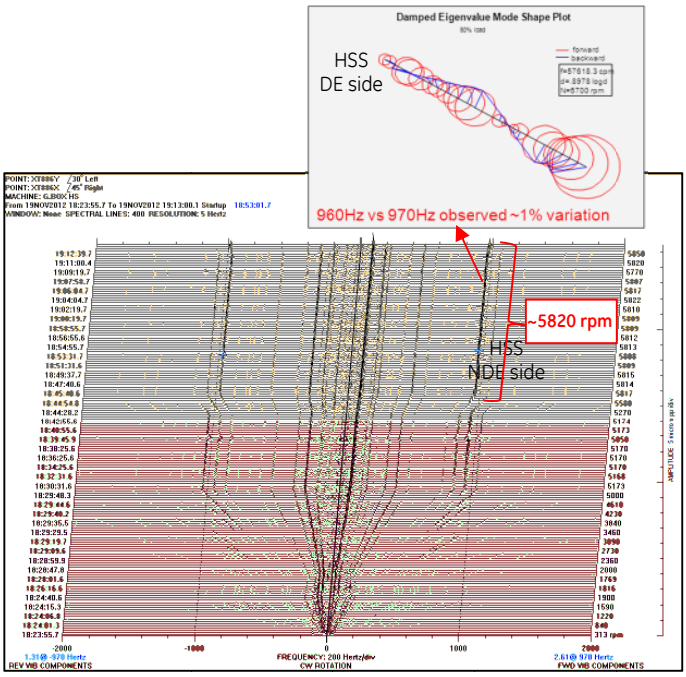

Figure 35 – Modified pinion - full Waterfall – HSS NDE "Y"

Moreover, the observed vibration characteristics in terms of whirl direction and amplitude are perfectly consistent with the calculation results: the forward whirl component is predominant and the vibration response with the modified pinion is much lower than the original case, due to the increased LogDec, in fact the maximum observed super-synchronous component is now 3 µm p-p @ 970 Hz.

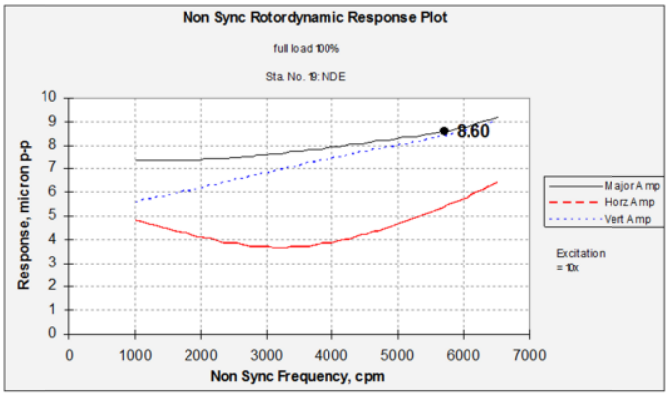

Figure 36 - Vibration response on NDE bearing location.

The figures 36 and 37 show the calculated vibration response at the NDE bearing centerline and NDE probe location, based on a rotor response analysis carried out using an explorative rotating force acting on the gear mesh, with a frequency of 10X speed harmonic.

This additional analysis has the aim to define the shaft vibration at the bearing center line starting from the measured vibration during the string test.

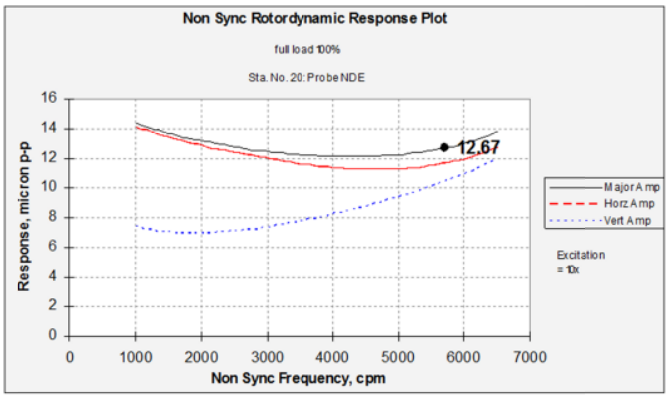

Figure 37 - Vibration response on NDE probe location.

The ratio between the vibration response at the probe location and the one at the bearing centerline is 12.67 / 8.6 = 1.47. Therefore, a vibration of 3 µm p-p detected by the no-contact probe corresponds to a vibration of roughly 2 µm p-p at the NDE bearing section (measured vibration dived by the calculated ratio).

PROPOSED METHOD OF 4TH MODE ANALYSIS

This section collects the main steps of the proposed method to study the gear rotors 4th lateral mode.

1 System Model Criteria

As described in the paragraph dedicated to the analysis of the modified pinion shaft (*Modified Rotor Analysis*), the system model procedure shall include the following steps:

1.1 The shaft beam model shall be in accordance to the FEM outcomes (tune the beam model to match the first and second free-free modes calculated by a FEM analysis).

1.2 The coupling components shall be modeled separately, including the flexible element; the polar and transversal moment of inertia shall be defined by a FEM analysis.

1.3 The bearing damping and the stiffness coefficients calculated at the frequency of interest (asynchronous coefficients), shall consider the system thermo-mechanical effects and the inertia effects in case of tilting pad journal bearing.

2 Lateral Analysis & Deliverables

2.1 The lateral study shall start with the analysis of the Undamped Critical Speed Map (UCS), in order to determine the shaft lateral natural frequency with the synchronous bearing stiffness.

2.2 Then, the study shall include the damping effects, using the bearing synchronous damping coefficients; the outcomes of this step shall be collected in a Campbell diagram showing the expected excitation harmonics, in order to define which of these natural frequencies shall be deeply investigated.

2.3 Finally, the analysis shall determine the damped eigenvalues for each of the critical natural frequency of interest, using the asynchronous bearing coefficients, in order to define its frequency, mode shape and modal damping. The analysis shall consider the different transmitted load conditions, based on the compressors operating points (if the different load will significantly change the 4th mode frequency, the analyst shall repeat the bearing super-synchronous coefficients calculation and then again recalculate the natural mode in order to converge through an iterative process).

3 Acceptance Criteria

Considering the analytical outcomes and the measurements results, the LogDec threshold which identify the critical area is 0.38, and therefore:

- LogDec ≥ 0.38 => low risk of high vibration response;
- LogDec < 0.38 => high risk of high vibration response;

Acceptability of the specific gear design shall be based on the proposed method, in case the analyzed gear falls in the critical area, it is strongly suggested to further investigate any design changes which would bring the system damping into the area of confidence.

CASES STUDY RESULTS - "D", "E" AND "F"

The cases "D", "E" and "F" point out successfully string tests results with the gearbox behavior consistent with the outcomes of the performed analysis with the proposed calculation method. The figures 38-41 depict the calculated pinion shaft 4th mode shape and LogDec for each of the mentioned cases.

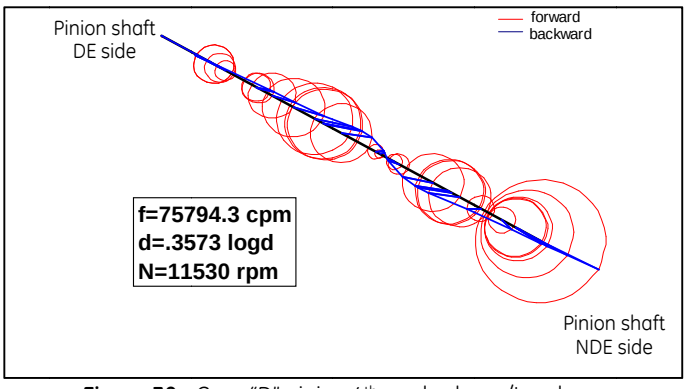

Figure 38 - Case "D" pinion 4th mode shape/Logdec

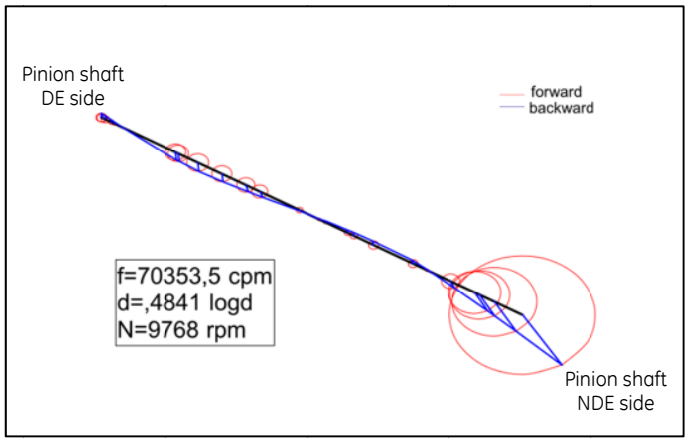

Figure 39 - Case "E" pinion 4th mode shape/Logdec

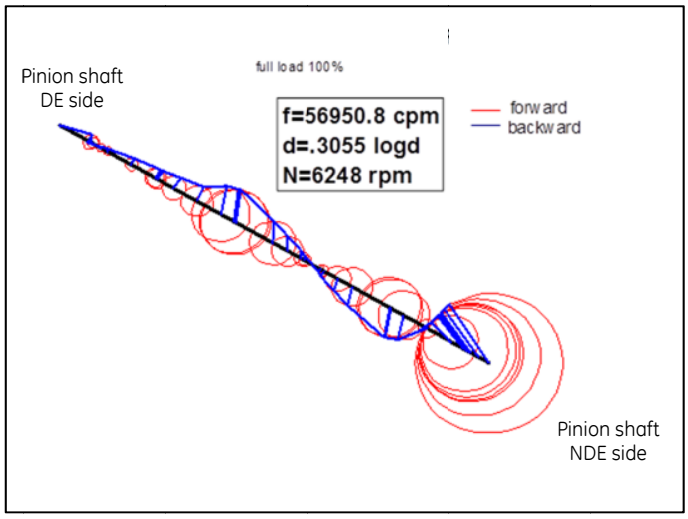

Figure 40 - Case "F" pinion 4th mode shape/Logdec (original design)

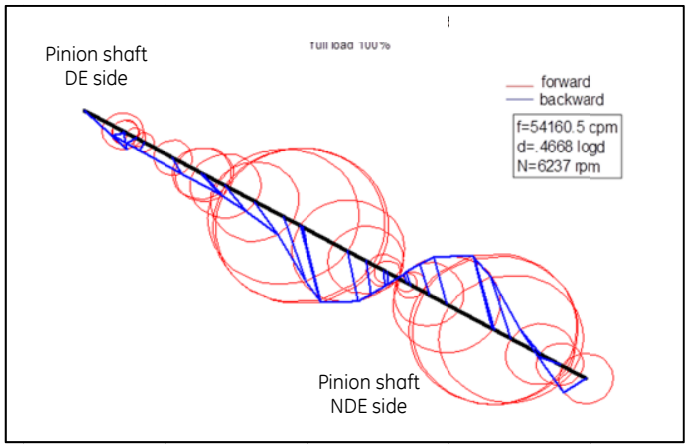

Figure 41 - Case "F" pinion 4th mode shape/Logdec (mod. Design)

The case "D" (Figure 38) point out a LogDec below the proposed acceptance criteria, even if really close to the area of confidence. A further sensitivity analysis versus load at the site operating conditions proved the goodness of original pinion shaft design.

The case "F" original design (Figure 40) had a 4th mode LogDec well below the acceptance criteria, thus leads to adopt the same pinion modification adopted in case "C". The modified pinion shaft improved the LogDec up to ~0.47 (compare the Figure 40 with the Figure 41).
Finally the good rotor-dynamic behaviour predicted by the calculation was confirmed by the positive results of the FSFL string test.

CONCLUSION

The paper details a series of experiences on super-synchronous vibration phenomena observed on geared systems. The authors develop a proven and reliable method to study and assess the gear super-synchronous behaviour during the design stage of the mechanical component. In addition to the lateral rotor-dynamic analysis required by API613, rotor super-synchronous analyses must be carried out to guarantee optimum gearbox behaviour during specific operating conditions.

A typical approach based on the separation speed margin cannot be used, since all shaft speed harmonics (7X, 8X, 9X, 10X, 11X, etc.) can excite a pinion 4th lateral mode in the operative speed range. This is even more critical in a variable speed drive application, where each of these shaft speed harmonics produces a wide speed range with potential to excite the super-synchronous behaviour.

In a trouble-shooting activity, where the operating speed range is already explored and active speed harmonics are identified, the pinion shaft could be modified to avoid the excitation mechanism. Nonetheless, it is much more effective having a method to assess the gear super-synchronous lateral behavior during the design phase.
The proposed method is based on the system modal damping, independent of the excitation source and its magnitude. If the system is well damped, the vibration response remains within an acceptable limit, which assures the correct operation of the gearbox during the performance test and the site service.

The new method of study is validated by several string test campaigns; in particular for case "C" at the authors' company, comprehensive tests confirm a good correlation between analytical outcomes and actual rotor dynamic behavior for both original and modified pinion shaft conditions.

Also of significant interest are the string test results for other published cases in the literature, "D", "E" and "F", which also validate the analytical model calculations and confirm the overall expectation.

ACKNOWLEDGMENTS

Special thanks go to Hans P. Weyermann Engineering Fellow, Rotating Equipment (ConocoPhillips Company), and Paul Bradley Technical Director (GE Allen Gears Company), for the contribution that they have provided to the writing of this paper.

NOMENCLATURE

FAT	Factory Acceptance Test
GT	Gas Turbine
GB	Gearbox
HSS	High Speed Shaft
LSS	Low Speed Shaft
PLV	Pitch Line Velocity
L/D	Length/Diameter
FSFL	Full Speed Full Load
FSNL	Full Speed No Load
FEM	Finite Element Model
NDE	Not Drive End
MCS	Maximum Continuous Speed
MOS	Minimum Continuous Speed
RCA	Root Cause Analysis
CMS	Component mode synthesis
WFR	Whirl Frequency Ratio
LogDec	Logarithmic Decrement
$a_{hx,y}$	Housing acceleration [m/s^2]
$A_{hx,y}$	Complex component of housing acceleration [m/s^2]
C_{ij}	Bearing damping coefficient [N.s/m]
$F_{x,y}$	Complex component of external forces [m/s^2]
H_{ij}	Dynamic impedance functions [N/m]
I	$\sqrt{-1}$
K_{ij}	Bearing stiffness [N/m]
M_h	Test housing mass [kg]
M_{ij}	Bearing mass coefficients [kg]
Ω	Excitation frequency [Hz]
Ω	Rotor speed [cpm]
x,y	Bearing dynamic motions in X,Y directions [m]
X,Y	Complex component of bearing motions [m]
UCS	Undamped Critical Speed

Subscripts

i,j	*X* and *Y* directions
H	Test housing

REFERENCES

API613 "Special Purpose Gear Units for Petroleum, Chemical and Gas Industry Services", Fifth Edition, American Petroleum Institute, Washington, DC.

API671 "Special Purpose Couplings for Petroleum, Chemical and Gas Industry Services", Fourth Edition, American Petroleum Institute, Washington, DC.

API684 "Tutorial on Rotor Dynamics: Lateral Critical, Unbalance Response, Train Torsional and Rotor Balancing", Second Edition American Petroleum Institute, Washington, DC.

[1] Edmund A. Memmott, 2006, "Case Histories of High Pinion Vibration When Eight Times Running Speed Coincides with the Pinion's Fourth Natural Frequency", MVA/ACVM 24th Machinery Dynamics Seminar.

[2] A. Delgado, M. Libraschi, G. Vannini, 2012, "Dynamic Characterization of Tilting Pad Journal Bearings From Component and System Level Testing", paper no. GT2012-69851, pp. 1007-1016, ASME Turbo Expo.

[3] T.W. Dimond, P.E. Allaire, A.A. Younan, P.N. Sheth, 2009, "Comparison of Tilting-Pad Journal Bearing Dynamic Full Coefficient and Reduced Order Models Using Modal Analysis", paper no. GT2009-60269, pp. 1043-1053, ASME Turbo Expo.

[4] T.W. Dimond, P.E. Allaire, A.A. Youna, 2012, "The Effect of Tilting Pad Journal Bearing Dynamic Models on the Linear Stability Analysis of an 8-Stage Compressor", J. Eng. Gas Turbines Power 134(5), 052503.

[5] H. Cloud, E.H. Maslen, L.E. Barrett, 2010, "Influence of Tilting Pad Journal Bearing Model on Rotor Stability Estimation", Eight IFToMM International Conference On Rotor Dynamics, MoB1-2, pp. 94-102.

[6] J.W. Lund, 1964, "Spring and Damping Coefficients for the Tilting Pad Journal Bearing", ASLE Transactions Volume 7, pp. 342-352.

[7] W. Shapiro, A. Colsher, 1977, "Dynamic Characteristic of Fluid-film Bearings", Proceedings of the Sixth Turbomachinery Symposium.
Turbomachinery Laboratory, Texas A&M University, College Station, Texas, pp. 39-53.

[8] L. Rodriguez, D. Childs, 2006, "Frequency Dependency of Measured and Predicted Rotordynamic Coefficients for Load-on-Pad Flexible-Pivot Tilting-Pad Bearings", Journal of Tribology, 128(2), pp. 388-395.

[9] A. Al-Ghasem, D. Childs, 2006, "Measurements Versus Predictions for a High Speed Flexure-Pivot Tilting-Pad Bearing (Load-Between-Pad Configuration)", Journal of Engineering for Gas Turbines Power, 128(4), pp. 896-906.

[10] C. Carter, D. Childs, 2008, “Measurements versus Predictions for the Rotordynamic Characteristics of a 5-Pad, Rocker-Pivot, Tilting-Pad Bearing in Load Between Pad Configuration”, ASME Paper GT2008-50069, Turbo Expo.

[11] E. J. Hensley, D, Childs, 2008, “Measurements Versus Predictions for Rotordynamic Characteristics of a Flexure Pivot-Pad Tilting Pad Bearing in an LBP Condition at Higher Unit Loads”, ASME Paper GT2008-50069, Turbo Expo.

[12] W. Dmochowski, 2007, “Dynamic Properties of Tilting-Pad Journal Bearings: Experimental and Theoretical Investigation of Frequency Effects Due to Pivot Flexibility", Journal of Engineering for Gas Turbines Power, 129(3), pp. 865-870.

[13] D. Childs, J. Harris, 2009, “Static Performance Characteristics and Rotordynamic Coefficients for a Four-Pad Ball-in-Socket Tilting Pad Journal Bearing”, Journal of Engineering for Gas Turbines Power, 131(6), 062502.

[14] J. Wilkes, 2011, “Measured and Predicted Transfer Function between Rotor Motion and Pad Motion for a Rocker-Back Tilting Pad Bearing in LOP Configuration”, ASME paper No. GT2011-46510, pp. 663-674.

[15] C. Rouvas, D. Childs, 1993, “A Parameter Identification Method for the Rotordynamic Coefficients of a High Reynolds Number Hydrostatic Bearing", ASME Journal of Vibration and Acoustics, 115, 264-270.

[16] B. H. Ertas, M. Drexel, J. Van Dam, D. Hallman, 2008, “A General Purpose Test Facility for Evaluating Gas Lubricated Journal Bearings”, ISROMAC, Proc of a Conference, Honolulu, Hawaii.

[17] J. Glienicke, 1966, “Experimental Investigation of Stiffness and Damping Coefficients of Turbine Bearings and Their Application to Instability Predictions", IMechE, Proceedings of the Journal Bearings for Reciprocating and Rotating Machinery, 181(3B), pp. 116-129.

[18] D. Childs, K. Hale, 1994, “A Test Apparatus and Facility to Identify the Rotordynamic Coefficients of High-Speed Hydrostatic Bearings”, Journal of Tribology, 116, pp. 337-334.

[19] P.E. Allaire, J.D Parsell, L.E. Barrett, “A Pad Perturbation Method for Tilting Pad Journal Bearing Dynamic Coefficients”, UVa Report No. UVA/643092/MAE81/183, University of Virginia, Charlottesville, Virginia.

[20] L. Branagan, L.E. Barret “Annex 4 – Tilting Pad Dynamic Coefficient Reduction with Pivot Flexibility”, UVa Report No. UVA/643092/MAE88/376, University of Virginia, Charlottesville, Virginia.

[21] “*Wear Control Handbook*” (eds. M.B. Peterson and W.O. Winer), ASME, 1980. Library of Congress No. 80-68846

[22] U. Baumann, 1999, “Rotordynamic Stability Tests on High-Pressure Radial Compressors”, Proceedings of the Twenty-Eighth Turbomachinery Symposium. Turbomachinery Laboratory, Texas A&M University, College Station, Texas, pp. 115 – 122.